ACS Macro Letters

Letter

pubs.acs.org/macroletters

Confinement of Acoustic Cavitation for the Synthesis of Protein-Shelled Nanobubbles for Diagnostics and Nucleic Acid Delivery

Meifang Zhou,[†] Francesca Cavalieri,[†,‡] Frank Caruso,*[,§] and Muthupandian Ashokkumar*[,†]

[†]School of Chemistry, The University of Melbourne, Parkville, Melbourne, Victoria 3010, Australia

[‡]Dipartimento di Scienze e Tecnologie Chimiche, Università di Roma Tor Vergata, 00173 Roma, Italy

[§]Department of Chemical and Biomolecular Engineering, The University of Melbourne, Parkville, Victoria 3010, Australia

Supporting Information

ABSTRACT: We report a novel flow-through sonication technique for synthesizing stable and monodispersed nano- and micrometer-sized bubbles that have potential applications in diagnostics and gene therapy. The size and size distribution of the bubbles are controlled by the active cavitation zone generated by ultrasound. These bubbles are shown to possess echogenic properties and can be used for loading oligonucleotides.

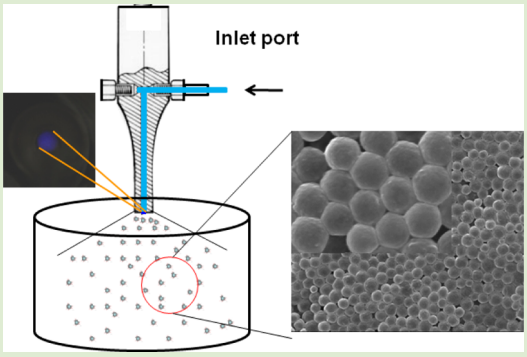

Microbubbles are uniquely suited as ultrasound contrast agents; however, they are typically too large to exit the vasculature and extravasate into tissue.[1−3] Recently, a microfluidic approach has been utilized to generate stable, monodisperse gas-filled microbubbles with controlled dimensions.[4−7] The MF technique, however, is limited to generating micrometer-sized gas bubbles, and the size distribution is time-dependent due to poor stability of the bubbles. The formulation of monodisperse theranostic *nano*bubbles holds immense potential in tumor imaging and therapy. The ability to synthesize nanobubbles has opened new opportunities to deliver therapeutic agents that require targeted extravasation from blood vessels into the tissues crossing the epithelial barriers such as the blood−brain barrier (BBB).[8,9] The formulation of nanobubbles with long-term stability, long circulation life, and narrow size distribution still remains a challenge. Although ultrasound has been widely reported for synthesizing microbubbles,[10,11] the size distribution of the ultrasonically synthesized microbubbles is significantly wider, and several experimental parameters affect the size and size distribution of microbubbles.[12,13] In this communication, we report a simple method to synthesize stable and relatively monodisperse nano- and microbubbles using a flow-through (FT) sonication technique. This is the first time that a FT system has been used to synthesize cross-linked stable nano- and microbubbles. This procedure can also be potentially applied to synthesize monodispersed nano- and microparticles.

The novelty of the FT technique lies in the fact that the active cavitation zone has been confined by choosing appropriate experimental conditions, in particular, the configuration of the ultrasonic horn. This approach is different to the commonly used ultrasonic spray dryers, where polydisperse and micrometer-sized, dried particles are generated.[14] The simple FT methodology that has been developed constitutes a platform offering versatility in the synthesis of nano- and microbubbles. We demonstrate that nanobubbles in the size range of 400−700 nm show echogenic properties and high loading capacities of oligonucleotides (1.6×10^3 DNA molecules/nanobubble).

Lysozyme, containing reactive thiol functional groups, was prepared as described previously.[15] To obtain lysozyme nano- and microbubbles, an aqueous solution containing partially denatured lysozyme was pumped through a 20 kHz FT horn at a flow rate of 175 mL/min and applied acoustic power of 240 W. Figure 1 shows a schematic representation of the method of formation of nano- and microbubbles using the FT sonication apparatus. The diameter of the horn tip was 1 cm, and the size of the hole, located in the middle of the horn, was 3 mm. The FT sonication can be run continuously by cycling the samples from the container. The protein solution was flowed through the middle of the horn using a peristaltic pump, and the horn was operated throughout the reaction time (continuous sonication). The solution was sprayed and collected in a glass container and recycled as required (Figure 1).

Figure 2 shows the size distribution and scanning electron microscopy (SEM) images of lysozyme nano- and microbubbles synthesized using standard and FT horns. It can be seen that narrow-sized nano- and microbubbles (stable for

Received: May 21, 2012
Accepted: June 18, 2012
Published: June 21, 2012

   dx.doi.org/10.1021/mz3002534 | *ACS Macro Lett.* 2012, 1, 853−856

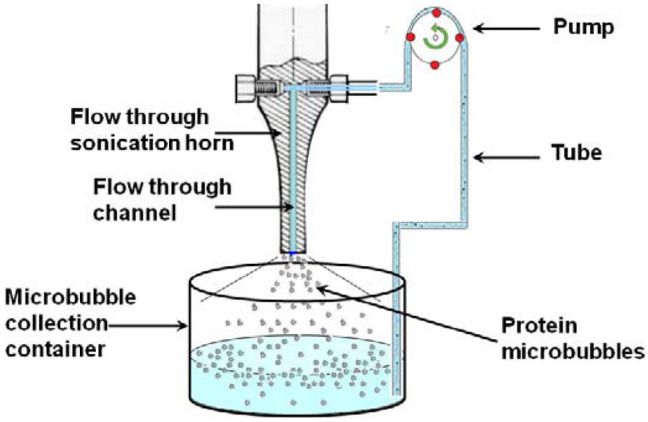

Figure 1. Schematic representation of the formation of nano- and microbubbles using the FT sonication cell.

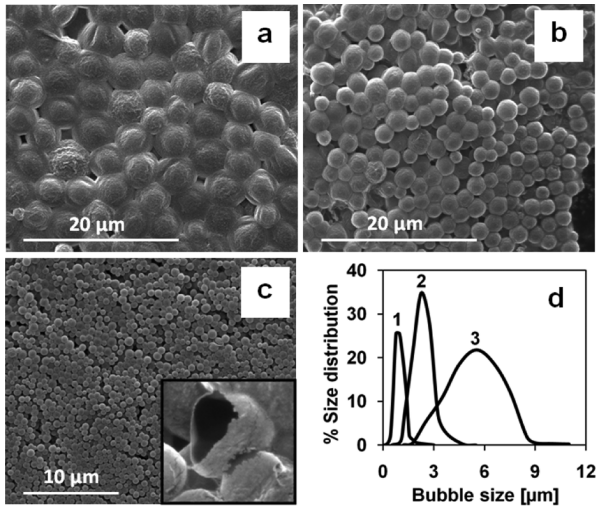

Figure 2. SEM images of lysozyme microbubbles synthesized using (a) a 1 cm standard horn (160 W), (b) a 3 mm standard horn (120 W), and (c) a flow-through horn (240 W). Inset (c): Broken nanobubbles. Size distribution of lysozyme bubbles (d): (1) a flow-through horn, (2) a 3 mm standard horn, and (3) a 1 cm standard horn.

several months) were generated by the FT process. To compare the size distribution of the bubbles generated by the FT method, bubbles were synthesized by the conventional (standard) ultrasonic method[12,15,16] using two different flat horn sonicators with tip diameters of 1 cm or 3 mm. It can be clearly seen in Figure 2 that the size and size distributions follow the order: 1 cm standard tip > 3 mm standard tip > FT horn. The smallest size (398 ± 10 nm) lysozyme-shelled bubbles were obtained with the FT sonication unit. This size and narrow size distribution could not be obtained using standard horns under a wide range of experimental conditions we examined.

Figure 2 shows that the diameter and type of horn affect the size and size distribution of the nano- and microbubbles. In our previous study,[12] we showed that the size and size distribution of sonochemically synthesized lysozyme-shelled microbubbles increased with an increase in acoustic power when a 3 mm standard horn tip was used. Considering the results shown in Figure 2 for standard horns with 1 cm and 3 mm diameters, the power density used for the 3 mm horn is significantly higher than that of the 1 cm horn (~200 W/cm^2 and 1700 W/cm^2 for 1 cm and 3 mm horns, respectively). While the observed differences in size and size distribution (Figure 2) could be due to the variation in acoustic power levels, our previous study[11] on the effect of acoustic power indicated that the size distribution widens at high power levels. If acoustic power was the controlling factor, then a wider size distribution should be observed with the 3 mm horn tip. However, the data in Figure 2 show a narrower size distribution for the 3 mm horn tip. Hence, the power density based on the size of the horn tip is not responsible for the observed size distributions shown in Figure 2.

An additional parameter that can be considered when using different types of horns is the active cavitation zone. Based on the proposed mechanism for nano- and microsphere formation,[10,11,15,16] the acoustic cavitation-generated emulsification process and radicals are crucial for microbubble formation. Applying acoustic power at the tip of a horn generates a cloud of cavitation bubbles at and around the horn surface (Figure 3). It can be expected that the power

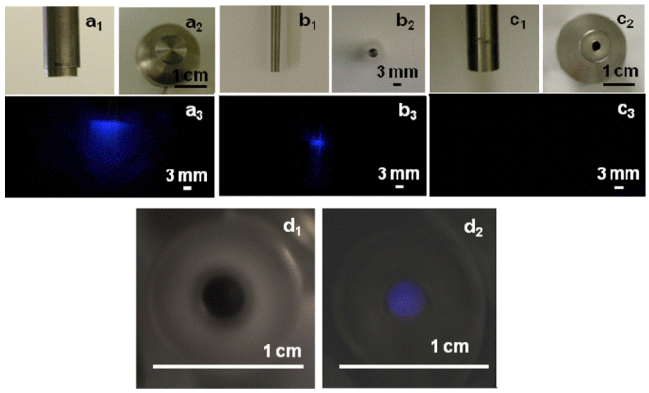

Figure 3. Photographs of horns and SCL images: (a) a_1 and a_2 are side and head-on views, respectively, and a_3 is a SCL image for a 1 cm horn; (b) b_1 and b_2 are side and head-on views, respectively, and b_3 is a SCL image for a 3 mm horn; (c) c_1 and c_2 are side and head-on views, respectively, and c_3 shows the (absence of) SCL image for a FT horn; (d) d_1 is an enlarged bottom (head-on) view, and d_2 a SCL image (head-on) for a FT horn.

distribution within this cavitation bubble cloud may be inhomogeneous:[13] the larger the active cavitation zone, the higher the inhomogeneity in power distribution. To examine if the "size" of the cavitation zone varied when the size of the horn tip was changed, a sonochemiluminescence (SCL) technique was used.[17] The active cavitation zone where OH radicals are generated during acoustic cavitation react with luminol, resulting in chemiluminescence. The active cavitation zones observed with 1 cm and 3 mm horn tips are shown in Figure 3. It is clear that the active cavitation zone observed with the 1 cm horn is significantly larger (area where sonochemiluminescence occurs is larger) than that observed with the 3 mm horn, despite the power density of the 3 mm horn being much higher (as mentioned earlier).

A comparison of the active cavitation zones of 1 cm and 3 mm tips to the size distributions observed for these horns (Figure 2) suggests that there may be a correlation between these two parameters. Based on this observation, it can be expected that the size distribution observed for the FT horn could be due to the confinement of the active cavitation zone to the hole region. Indeed, the active caviation zone is limited to

dx.doi.org/10.1021/mz3002534 | ACS Macro Lett. 2012, 1, 853−856

the hole region, as shown in Figure 3. When we attempted to photograph the active caviation zone from the side (as for the standard horn systems), no SCL could be observed. When the camera was placed at the bottom facing the horn tip, an active cavitation zone that is limited to the hole region (the active zone is 2-dimensional rather than 3-dimensional as in standard horns) could be observed. One can also expect acoustic cavitation inside the hole when liquid flows through. However, we speculate that the nano- and microbubbles are formed only at the surface of the hole where an air−liquid interface exists. It has been shown in previous studies that microbubbles are generated only when the horn is placed at an air−liquid interface.[18]

To demonstrate the versatility of the FT sonication method to synthesize nano- and microbubbles stabilized with different materials, thermally denatured bovine serum albumin, BSA, was used instead of lysozyme. The overall trend in the size distribution was found to be similar to that of lysozyme bubbles. The average size of BSA bubbles is reduced from 850 nm to 1.2 μm for the 3 mm tip to 550−650 nm for the FT unit.

Another aim of our study was to produce stable nanobubbles to use as a viable ultrasound contrast agent. Nanobubbles are considerably less effective scatterers of ultrasound due to the sixth power radius dependence of the Rayleigh scattering.[19] The resonance frequency of the nanobubbles is expected to be much higher than that of microbubbles. To determine the ability of the bubbles to generate backscattered ultrasound signals, the ability of the synthesized nanobubbles as contrast agents to enhance ultrasound images using a 10 MHz scanner was investigated.

We used a phantom as a tissue-mimicking structure (see Supporting Information). Two channels were made within the phantom as special channels for nanobubble liquid flowing through. A lysozyme aqueous solution (1 mg mL^{-1}) was injected as a reference into one channel, and a lysozyme nanobubble solution (10^7 nanobubbles mL^{-1}) was injected into a second channel. An ultrasound probe was then used on the phantom at 10 MHz with a mechanical index at 0.36. The ultrasound scanning images show that the channel with lysozyme microbubble solution appears as a black hole both in B- and color modes (Figure 4a and b), showing no backscattering from the solution. The channel with lysozyme nanobubbles shows bright particles moving within the hole (Figure 4c) under the B-mode, and a uniform blue hole (Figure 4d) appears when operating under the color mode. This shows that the backscattered signals are caused by lysozyme nanobubbles.

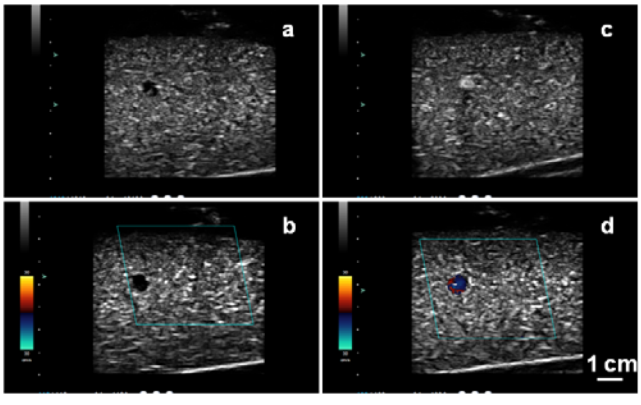

Figure 4. Sonographic images of a tissue mimicking phantom injected with (a) lysozyme aqueous solution in B-mode; (b) color mode; and nanobubbles dispersed in water in (c) B-mode and (d) color mode.

To prepare that the synthesized nanobubbles for possible DNA delivery applications, double-stranded (ds) oligonucleotides were loaded onto lysozyme nanobubbles (Figure 5). In principle, the radiation force generated by sonication in vivo can drive the systemically administered nanobubbles toward pores (380−780 nm) in the leaky angiogenic tumor vessels and induce penetration of nanobubbles through the pores.[20,21]

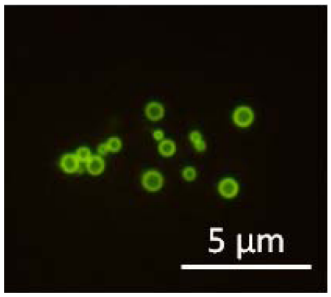

Figure 5. Fluorescence optical microscopy image of DNA-loaded lysozyme nanobubbles. Picogreen, a DNA intercalating fluorochrome, was used to stain the ds oligonucleotides.

The highly charged nanobubble surface and shell are suitable for the adsorption of nucleic acids, resulting in protein−DNA complex formation. The microbubble shell is around 80 nm thick (see Figure 2). The ds oligonucleotide (0.5 μM) was incubated with the nanobubble suspension (1.5 mg mL^{-1}). The loaded nanobubbles maintain their integrity (Figure 5), and each nanobubble has the capacity to load 1600 ds oligonucleotides (see the Supporting Information).

In summary, we have established a novel and facile platform to synthesize stable and relatively monodispersed bubbles with diameters in the nano- to micrometer range. The size of the nano- and microbubbles is controlled by the active cavitation zone. The nanobubbles formed were found to possess echogenic properties and drug-loading capacity. The FT technique produces stable nano- and microbubbles due to the covalent links formed between protein molecules by acoustic cavitation generated radicals. In addition, large quantities of uniformly sized stable nano- and microbubbles can be generated at a relatively low cost using the FT method, due to its simple operation procedure.

■ ASSOCIATED CONTENT

Ⓢ Supporting Information

Experimental details. This material is available free of charge via the Internet at http://pubs.acs.org.

■ AUTHOR INFORMATION

Corresponding Author

*M.A.: Fax: +61-3-93475180; tel.: +61383447090; e-mail: masho@unimelb.edu.au. F.C.: Fax: +61-3-8344 4153; tel.: +61-3-8344 3461; e-mail: fcaruso@unimelb.edu.au.

Notes

The authors declare no competing financial interest.

■ ACKNOWLEDGMENTS

The authors acknowledge the financial support from the Australian Research Council under the under the Federation Fellowship (F.C.) and Discovery Project (M.A.) schemes.

■ REFERENCES

(1) Cosgrove, D.; Harvey, C. *Med. Biol. Eng. Comput.* **2009**, *47*, 813−826.
(2) Ferrara, K.; Pollard, R.; Borden, M. *Annu. Rev. Biomed. Eng.* **2007**, *9*, 415−447.
(3) Qin, S.; Caskey, C. F.; Ferrara, K. W. *Phys. Med. Biol.* **2009**, *54*, R27−57.
(4) Hettiarachchi, K.; Talu, E.; Longo, M. L.; Dayton, P. A.; Lee, A. P. *Lab Chip* **2007**, *7*, 463−468.
(5) Park, J. I.; Tumarkin, E.; Kumacheva, E. *Rapid Commun.* **2010**, *31*, 222−227.
(6) Park, J. I.; Jagadeesan, D.; Williams, R.; Oakden, W.; Chung, S.; Stanisz, G. J.; Kumacheva, E. *ACS Nano* **2010**, *4*, 6579−6586.
(7) Seo, M.; Gorelikov, I.; Williams, R.; Matsuura, N. *Langmuir* **2010**, *26*, 13855−13860.
(8) Kinoshita, M.; McDannold, N.; Jolesz, F. A.; Hynynen, K. *Proc. Natl. Acad. Sci. U.S.A.* **2006**, *103*, 1719−11723.
(9) Liu, H. L. *Radiology* **2010**, *255*, 415−425.
(10) (a) Suslick, K. S.; Grinstaff, M. W. *J. Am. Chem. Soc.* **1990**, *112*, 7807−7809. (b) Dibbern, E. M.; Toublan, F. J.-J.; Suslick, K. S. *J. Am. Chem. Soc.* **2006**, *128*, 6540−6541.
(11) (a) Gedanken, A. *Chem.—Eur. J.* **2008**, *14*, 3840−3853. (b) Grinberg, O.; Hayun, M.; Sredni, B.; Gedanken, A. *Ultrasonics Sonochem.* **2007**, *14*, 661−666.
(12) Zhou, M.; Cavalieri, F.; Ashokkumar, M. *Soft Matter* **2011**, *7*, 623−630.
(13) Han, Y.; Radziuk, D.; Schukin, D.; Moehwald, H. *J. Mater. Chem.* **2008**, *18*, 5162−5166.
(14) Freitas, S.; Merkle, H. P.; Gander. *J. Controlled Release* **2004**, *95*, 185−195.
(15) Cavalieri, F.; Ashokkumar, M.; Grieser, F.; Caruso, F. *Langmuir* **2008**, *24*, 10078−10083.
(16) Cavalieri, F.; Zhou, M.; Caruso, F.; Ashokkumar, M. *Chem. Commun.* **2011**, *47*, 4096−4098.
(17) Sunartio, D.; Yasui, K.; Tuziuti, T.; Kozuka, T.; Iida, Y.; Ashokkumar, M.; Grieser, F. *ChemPhysChem* **2007**, *8*, 2331−2335.
(18) Grinstaff, M. W.; Suslick, K. S. *Proc. Natl. Acad. Sci. U.S.A.* **1991**, *88*, 7708−7710.
(19) Morse, P. M.; Ingard, K. U. *Theoretical Acoustics*; McGraw Hill: New York, 1968.
(20) Li, W. W. *Acad. Radiol.* **2000**, *7*, 800−811.
(21) Pasqualini, R.; Arap, W.; McDonald, D. M. *Trends Mol. Med.* **2002**, *8*, 563−571.